Reversible Inactivation of Human Dipeptidyl Peptidases 8 and 9 by Oxidation

Joohong Park[†,1], Heather M. Knott[#,1], Naveed A. Nadvi[1,3], Charles A. Collyer[4], Xin M. Wang[1], W. Bret Church[3] and Mark D. Gorrell*[,1,2]

[1]*Centenary Institute, Faculty of Medicine, The University of Sydney,* [2]*A. W. Morrow Gastroenterology and Liver Centre, Royal Prince Alfred Hospital,* [3]*Pharmaceutical Chemistry, Faculty of Pharmacy, The University of Sydney and* [4]*Molecular and Microbial Biosciences, Faculty of Science, The University of Sydney*

Abstract: Hydrogen peroxide (H_2O_2) can act as an intracellular messenger by oxidizing sulfhydryl groups in cysteines that can be oxidized at neutral pH. The oxidizing agents H_2O_2 and pyrroloquinoline quinone and the large thiol reagents N-ethylmaleimide and 4-(hydroxymercuri) benzoate each inhibited dipeptidyl peptidase (DP) activity in the intracellular DPIV-related proteins DP8 and DP9 at pH 7.5. In contrast, these treatments did not alter activity in DPIV and fibroblast activation protein. Peptidase inhibition was completely reversed by 2-mercaptoethanol or reduced glutathione. Alkylation of DP8 by the small thiol reagent iodoacetamide prevented inhibition by H_2O_2, N-ethylmaleimide or pyrroloquinoline quinone. Two cysteines were reactive per peptidase monomer. We exploited these properties to highly purify DP8 by thiol affinity chromatography. Homology modelling of DP8 and DP9 was consistent with the proposal that the mechanism involves decreased protein flexibility caused by intramolecular disulfide bonding. These novel data show that DP8 and DP9 are reversibly inactivated by oxidants at neutral pH and suggest that DP8 and DP9 are H_2O_2 sensing proteins.

Key Words: Redox regulation, H_2O_2, Cysteine, Dipeptidyl peptidase, Fibroblast activation protein, Prolyl oligopeptidase, Hydrogen peroxide sensing.

INTRODUCTION

Hydrogen peroxide (H_2O_2) as an intracellular messenger is a mild oxidant that in target proteins can oxidize sulfhydryl groups in cysteine (Cys) residues (Cys-SH) to Cys sulfenic acid (Cys-S-OH), which can then disulfide bond with a neighboring Cys. Generally, Cys residues in proteins have a pKa> 8.0 and so most of them are in protonated forms at physiological pH. However, a few proteins have been found to contain reactive Cys residues, probably potentiated by positive charges from nearby amino acids, that have a pKa < 7 and so can be oxidized at or below neutral pH [1-3]. Due to the intracellular presence of millimolar glutathione (GSH), oxidized Cys residues become reduced. Signal transduction by reactive Cys modification of protein tyrosine phosphatases and phosphatase and tensin homolog (PTEN) is involved in insulin and growth factor signalling [4-7]. However, few H_2O_2 sensing proteins have been identified [8, 9]. In contrast to intracellular proteins, in extracellular proteins most Cys residues are in disulfide bonds.

Enzymes of the S9 or prolyl oligopeptidase family, which includes prolyl endopeptidase (PEP) and the dipeptidyl peptidase (DP) IV subfamily, have the rare enzyme ability to hydrolyse a post-proline bond. DPIV family enzymes can hydrolyse such a prolyl bond that is two residues from the N-terminus of substrates [10]. The DPIV enzyme family consists of DPIV, fibroblast activation protein (FAP), DP8 and DP9. Much interest has been focused on the enzyme activity of DPIV, and its inhibition as a type 2 diabetes therapy [11], but DPIV has roles in metabolism, immune responses, the endocrine system and cancer biology. FAP has roles in liver and cancer biology [12]. No *in vivo* functions of DP8 and DP9 have been delineated. Identification of DP8 and DP9 as enzymes possessing DPIV enzyme activity, previously assumed unique to DPIV, has stimulated investigations of DP8/9 functions and enzyme activity. Such knowledge is crucial for further progress in understanding the biological issues surrounding selective targeting of DPIV family enzymes for disease therapies.

Even though there is about 27% amino acid identity among the DPIV enzyme family members and 17% identity with PEP [13], some differences in structure and function may relate to subcellular location. The intracellular proteins PEP, DP8 and DP9 have a different chemical environment to the extracellular proteins DPIV and FAP. In DPIV, most disulfide bonds appear to have a structural role [14, 15]. However, the roles of Cys in DP8 or DP9 are unknown. The chemical modification of PEP Cys residues with thiol reagents has shown that a Cys is sufficiently near to the active site that a large thiol reagent, N-ethylmaleimide (NEM) or 4-(hydroxymercuri) benzoate (pHMB), excludes the substrate whereas a smaller molecule, iodoacetamide (IAA), does so only partially [16]. In the three-dimensional (3D) structure of PEP Cys255 is situated close to the S1 and S3 subsites such that a covalent bond from this Cys to large alkylating reagents can block substrate passage [17].

In this study, we investigated the functionality of Cys residues in the DPIV family. Treating DPIV and FAP with alkylating, oxidising or reducing agents did not alter their

*Address correspondence to this author at the Centenary Institute, Locked Bag No. 6 Newtown, NSW 2042, Australia; Tel: 61 2 95656100; Fax: 61 2 95656101; E-mail: m.gorrell@centenary.usyd.edu.au

†Department of Medicine (Dermatology), The University of Sydney

#The Heart Research Institute, Sydney

1874-9402/08

enzyme activities. In contrast, DP8 and DP9 exhibited less peptidase activity following oxidation or thiol alkylation. Moreover, reducing agents completely reversed this oxidation mediated enzyme activity abrogation. Enumerating the thiols and observing electrophoretic mobility under non-reducing conditions suggested that intramolecular disulfide bond formation in DP8 and DP9 regulates the peptidase activity of these proteins.

MATERIALS AND METHODS

Reagents

Iodoacetamide (IAA), pHMB, NEM, pyrroloquinoline quinone (PQQ), 2-mercaptoethanol (2-ME), dithiothreitol, reduced glutathione (GSH) and Ellman's reagent [18], 5,5'-dithiobis(2-nitrobenzoic acid) (DTNB), were purchased from Sigma Aldrich (St Louis, MO).

Proteins

The proteins expressed in this study were human DP8 (882 residues; GenBank AF221634), human DP9 (863 residues; GenBank AY374518), human DPIV (GenBank M80536) and human FAP (GenBank U09278). The extracellular portions of DPIV (739 residues) and FAP (722 residues) were made, starting at residues Leu28 in DPIV and Met39 in FAP. The four prolyl oligopeptidase family members were expressed with polyhistidine (6xHis) C-terminal tags using the pMelbac baculovirus expression system and *Spodoptera frugiperda* 9 cells [19]. DPIV, DP9 and FAP were purified by metal affinity chromatography [19]. DP8 purification used CM cation exchange and DEAE Sephacel anion exchange because the polyhistidine on DP8 did not bind to the metal resin unless it was denatured.

For purification of DP8, solid $(NH_4)_2SO_4$ was added to insect cell culture supernatant, discarding the 40% cut and retaining the 80% saturation precipitate. The purification of DP8 then used CM cation exchange chromatography, Blue Sepharose chromatography and DEAE Sephacel anion exchange chromatography with these column media from Amersham. CM Sepharose was equilibrated with 10 mM sodium phosphate pH 5.5. Bound protein was eluted by increasing salt concentration up to 150 mM. Active fractions were applied to Blue Sepharose then DEAE Sephacel, both equilibrated with 10 mM sodium phosphate pH 7.6. Bound proteins were eluted from DEAE Sephacel by increasing the NaCl concentration stepwise to 200 mM.

Protein concentrations were measured by the Bradford method and purity assessed by silver stained SDS-PAGE. Western blots used a mouse antibody to C-terminal polyhistidine (Invitrogen, CA), mouse monoclonal anti-FAP antibody F19 (CRL-2733, ATCC), biotinylated rabbit anti-mouse antibody (Dako, CA) and streptavidin HRP (Dako, CA) [20]. Identification of the four purified enzymes was confirmed by Edman N-terminal degradation at the Australian Proteome Analysis Facility. The DPIV enzyme activity of DPIV, DP8, DP9 and FAP was measured using H-Ala-Pro-pNA in the DPIV assay described previously [21].

Titration of Cys

1×10^{-3} M Ellman's reagent was made by dissolution in about 1 ml 95% ethanol then dilution with 0.1 M Tris buffer pH 7.6. Thiols were determined spectrophotometrically at 412 nm, using an extinction coefficient for thionitrobenzoate of 13,600 M^{-1} cm^{-1}, before and after the addition of 6 M guanidine HCl to the enzymes DP8 and DPIV. Absorption measurements were made with a Perkin Elmer (Waltham, MA) Model Lambda 3B UV-visible spectrophotometer, using 1 cm path length quartz cuvettes.

Bioinformatics

Homology modelling of DP9 and DP8 used the protein crystal structures of DPIV, DP6 and FAP (1N1M; 2.5 Å [15], 1XFD; 3.0 Å [22] and 1Z68; 2.6 Å [23] respectively) from the Protein Data Bank [24] and a multiple sequence alignment of fifty proteins of the prolyl oligopeptidase gene family [25]. This multiple sequence alignment upon which our structural assessments were based had been created previously without any preconceptions that would prejudice our final interpretations. The PDB entries for DPIV, DP6 and FAP start at residues Ser39, Gln127 and Met39 respectively and so that the termini beyond the locations of the template structures were not considered the N-termini of the 882 and 863 amino acid forms of DP8 and DP9 were N-terminally truncated at the equivalent locations in the alignment to begin at residues Lys62 and Lys51, respectively. Similarly, eight C-terminal residues of DP8 were removed in order to model structure at the C-terminus that is available directly from the template. The truncated sequences of DP8 and DP9, and modified template structures (only chain A and no HET atom records) were used as input for the comparative protein modelling software MODELLER [26], using the graphical user interface of Discovery Studio (DS) (v1.7, Accelrys, San Diego, CA, USA). Briefly, the template structures were aligned using ALIGN3D, and the DP8 and DP9 sequences were aligned to the structurally aligned templates using ALIGN2D. This alignment preserved all the structural features of our previous more extensive alignment [25]. Modelling used high optimization settings and loop refinement.

Model validation used PROCHECK [27]. The percentage outliers in the Ramachandran plots in the most-favoured and additional allowed regions was 4.3% for the DP8 model and 2.4% for the DP9 model, while the values for the templates DP4, DP6 and FAP were 2.2%, 3.7% and 0.8% respectively. All significant secondary structure and the catalytic triad had close correspondence between the templates and models. Model veracity was further suggested by considering known features. In the DP9 model the two potentially glycosylated asparagines, Asn205 and Asn653, were solvent-exposed. The residues that align with the natural cleavage site of DPIV at Ala282 in the blade 4 β3-β4 loop [28] were located on equivalent loops in both models. DPIV Val341 that is essential for binding to the ligand adenosine deaminase [29] aligns in both models with valines in the blade 5 β3-β4 loop. Moreover, His750, which is essential for DPIV dimerisation [30], is conserved in all the templates and models. Protein structure visualization and Cα-Cα measurements used PyMOL [31].

RESULTS

Alignment of Cys Residues in the DPIV Family

There is approximately 27% amino acid identity among the DPIV enzyme family members [13]. However, the intracellular proteins DP8 and DP9 show marked differences in

Table 1. Cys Conservation in the Human DPIV Enzyme Family. The amino acids aligning with each Cys of DP9 in the DPIV gene family members DP8, DPIV and FAP in a 50-protein multiple sequence alignment [25] and in PEP. A dash indicates that no residue aligned. Total number of Cys per monomer subunit is shown in brackets

DP9 (14)	DP8 (12)	DPIV (12)	FAP (12)	PEP (16)
Cys 162	Val 173	Ile 134	Ile 132	Phe 132
Cys 184	Cys 195	-	-	Ser 144
Cys 194	Cys 205	Thr 152	Ile 150	Ser 148
Cys 225	Val 236	Tyr 183	Phe 181	Trp 178
Cys 259	Cys 270	Ser 217	Ser 215	Thr 204
Cys 440	Glu 449	Ser 370	Ser 353	-
Cys 447	Cys 456	-	-	-
Cys 452	Arg 461	Glu 379	Asp 362	-
Cys 481	Cys 490	Trp 402	Trp 395	Gly 369
Cys 550	Cys 559	-	-	-
Cys 571	Cys 580	Leu 477	Ile 471	Gly 405
Cys 601	Pro 610	Gln 505	Lys 499	Asp 431
Cys 683	Cys 692	Gly 584	Ala 578	Gly 508
Cys 844	Val 853	Ser 744	Ser 737	Ala 685

primary protein structure in terms of Cys locations when compared to the membrane-bound proteins FAP and DPIV (Table **1**). Eight of the 14 Cys in DP9 have similar locations in DP8, but no Cys location was seen to be conserved throughout the DPIV gene family. This observation suggests that Cys functions may differ in DP8 and DP9 compared to DPIV and FAP.

Effects of Thiol Specific Reagents on DPIV Enzyme Activity

Protein purity was verified ([19], Figs. **1** and **2**). The specific activities of purified DPIV, DP8, DP9 and FAP were 21.2, 1.8, 4.1 and 8.9 Units/mg respectively.

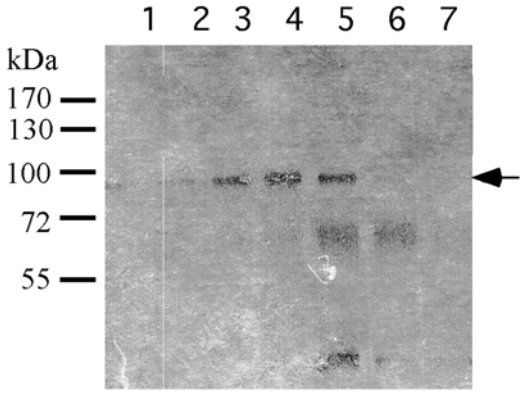

Fig. (1). Purification of recombinant human DP8. Silver stained 8% SDS-PAGE of some fractions eluted from DEAE Sephacel anion exchange chromatography. Arrow indicates intact DP8. Some fractions, including lane 5, contained both intact DP8 and DP8 fragments. Samples were heated to monomerise dimers.

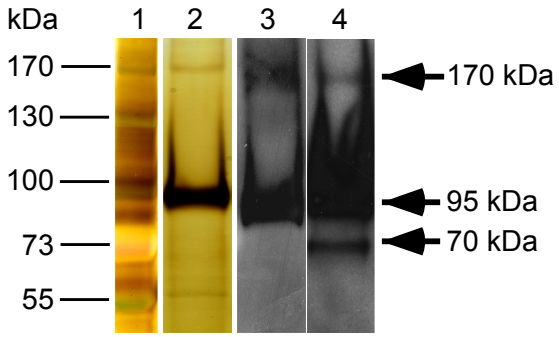

Fig. (2). Purification of recombinant human FAP. Analysis of purified FAP protein by silver stained 8% SDS-PAGE (Lane 2) and by Western blot using anti-FAP antibody F19 (Lane 3) and anti-6xHis antibody (Lane 4, overloaded to visualize dimer). Monomeric FAP runs at 95 kDa and dimeric FAP at 170 kDa [20]. The 70 kDa band is probably a FAP fragment. Lane 1: molecular mass standards. Samples were not heated.

Thiol specific compounds of different sizes were allowed to react with DPIV, FAP, DP8 and DP9 at 10 μM (Fig. **3**). DP9 was inhibited 45%-50% by the small thiol reagent iodoacetamide (IAA) (Fig. **3**). In contrast to DP9 and concordant with our previous results [32], IAA caused no inhibition of DP8. However, the dipeptidyl peptidase activity of both DP8 and DP9 was inhibited by larger thiol compounds. 4 pHMB completely inhibited DP8 and DP9 catalytic activity. NEM was also a very effective inhibitor of these two peptidases (Fig. **3**). The time course data of NEM and pHMB on DP8 and DP9 fitted nonlinear regressions with R values > 0.97.

To obtain evidence that IAA and NEM react with the same thiol group, NEM (2 mM) was added to DP8 following

IAA treatment. No significant additional inactivation by NEM of IAA - pretreated DP8 was observed, whereas without IAA pretreatment NEM decreased DP8 activity by about 80% (Fig. **4**). DPIV and FAP were not inhibited by any of the thiol reagents (Figs. **3** and **5**).

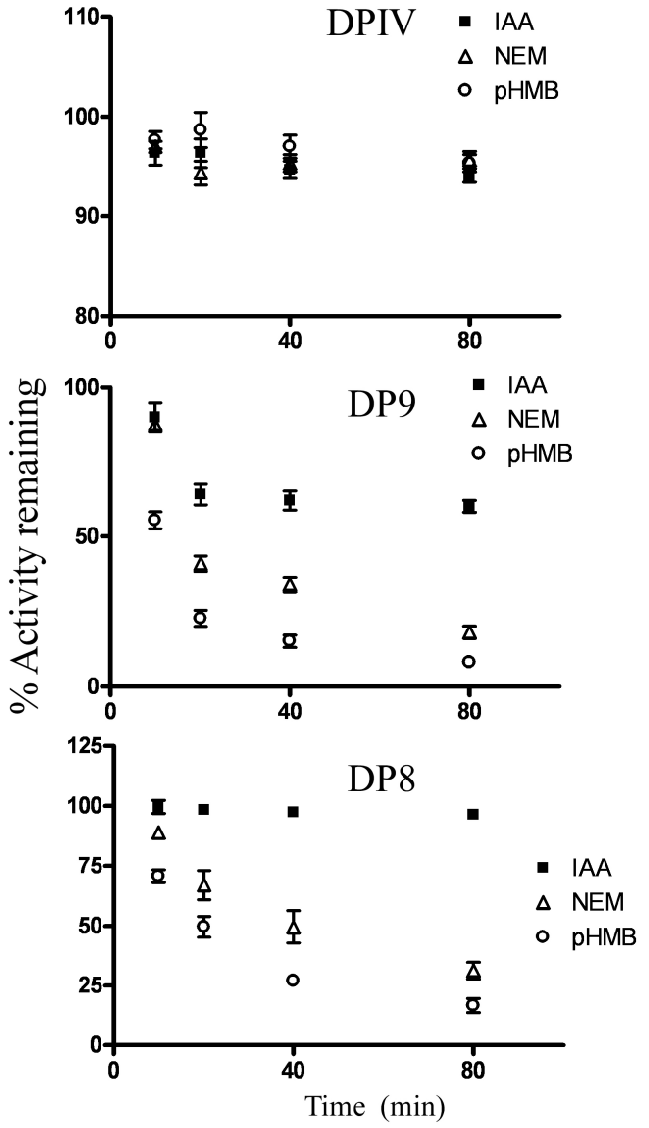

Fig. (3). Effect of thiol-specific reagents on enzyme activity in the DPIV family. Purified DPIV, DP9, or DP8 at 10 μM were incubated with IAA (10 mM), NEM (2 mM) or pHMB (0.5 mM) for a series of time periods then assayed using substrate H-Ala-Pro-pNA. Controls included untreated enzymes. Mean and SD, n = 4.

Oxidation of DP8 and DP9 Thiol Residues

H_2O_2 is a small molecule that can oxidize Cys residues to Cys sulfenic acid or disulfide. As a coenzyme of several bacterial dehydrogenases, PQQ [33] catalyzes the oxidation of vicinal cysteinyl residues to generate disulfide bonds under mild experimental conditions such as thioredoxin, phosphoribulose kinase, and 4-aminobutyrate aminotransferase [34]. The two oxidizing agents H_2O_2 and PQQ were used to test the possibility that the peptidase activity of DP8 and DP9 diminishes upon oxidation of thiol residues (Fig. **6**). 80% loss of dipeptidyl peptidase activity was observed by incubating the enzyme at 10 μM with H_2O_2 at 0.2 mM for 100 min at 37°C in 0.1 M sodium phosphate buffer pH 7.5. PQQ at 0.2 mM inhibited activity by 70% after 80 min at 37°C in pH 7.5 sodium phosphate buffer. The inhibition pattern of DP9 was similar to that of DP8 (Fig. **6**). The inhibition was both time and dose dependent, with data fitting nonlinear regressions with R values > 0.95. No inhibition of DPIV and FAP by H_2O_2 was seen.

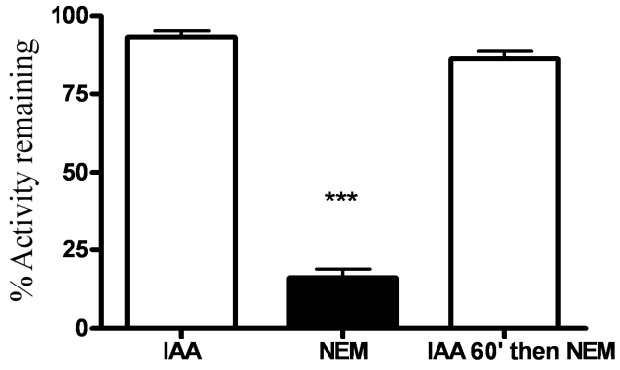

Fig. (4). Interaction of thiol reagents with DP8. Iodoacetamide (IAA) pretreatment of DP8 prevented inhibition by NEM. Samples of DP8 (10 μM) were incubated with IAA (10 mM) or NEM (2 mM) for 1 h at 37°C in 0.1 M pH 7.5 sodium phosphate buffer, or DP8 was incubated with IAA before NEM treatment. The samples were passed through a Sephadex-G25 column to remove IAA and NEM prior to assay with substrate H-Ala-Pro-pNA. Data are mean ± SD of three independent experiments performed in triplicate. Statistical analysis used Student's t test. ***$p<0.001$ for IAA - treated compared to NEM - treated DP8.

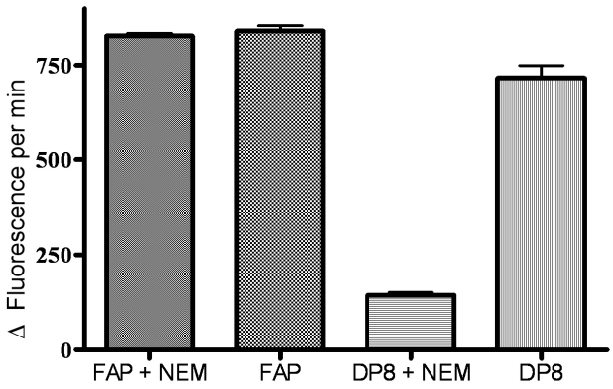

Fig. (5). FAP is unaffected by the large thiol-specific reagent NEM. Purified FAP and DP8 were incubated with NEM (2 mM) or control buffer for 30 min then assayed using the DP substrate H-Ala-Pro-7-amido-4-trifluoromethylcoumarin (AFC). Enzyme activity was expressed as arbitrary units of fluorescence (510 nm) change per minute.

To ascertain whether thiol reagents and oxidizing agents react with the same thiol group, DP8 was alkylated before exposure to oxidizing agents and thiol groups were titrated using DTNB at 1 mg/ml in the presence of 6 M guanidine-HCl. DP8 alkylated by IAA was resistant to inactivation by H_2O_2 or PQQ. Six SH residues of active DP8 reacted with DTNB reagent. However, both IAA pretreated DP8 having

enzyme activity and DP8 oxidized by either H_2O_2 or PQQ, which cause inactivation showed four SH residues reactive to DTNB. The spectrophotometric measurements indicate the oxidation of approximately two SH residues per enzyme monomer (Table **2**).

Redox Reversibility of Enzyme Activity

Samples of oxidized DP8 were preincubated with the reducing agents 2-ME, dithiothreitol or GSH. As shown in Fig. **7**, recovery of catalytic activity was achieved in the presence of 12.8 mM 2-ME or 5 mM GSH for both DP8 and DP9.

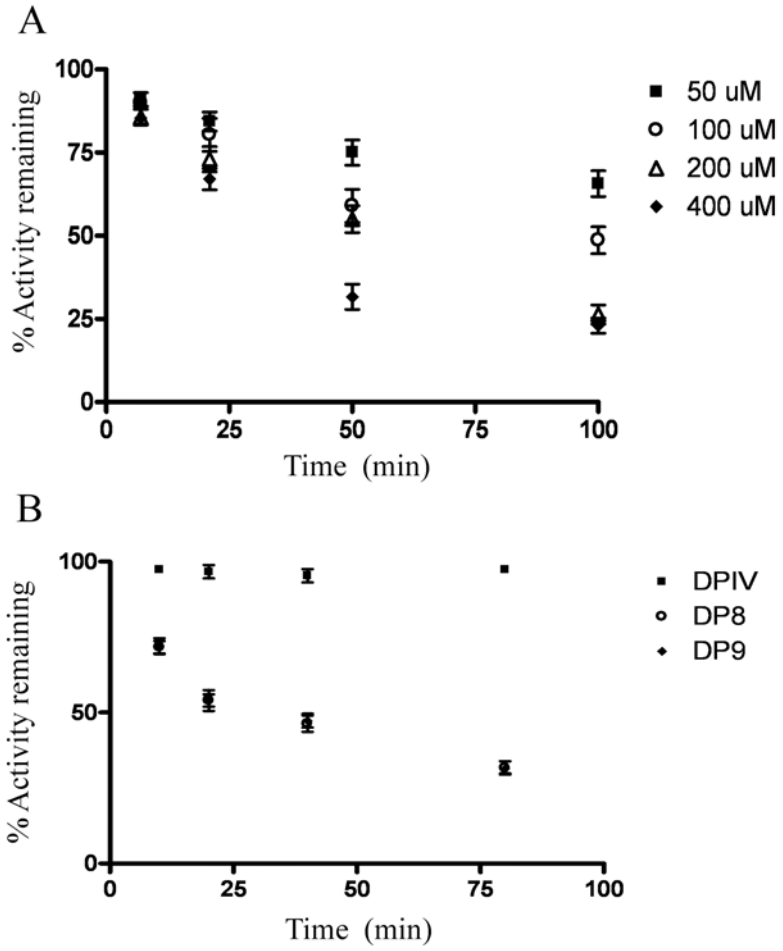

Fig. (6). Time and dose responsiveness to oxidizing agents of enzyme activity in the DPIV family. **A.** Time course of inactivation of purified DP8 with different concentrations of H_2O_2. **B.** Time course of inactivation of purified 10 μM DP8 and 10 μM DP9 by 0.2 mM PQQ. Dipeptidyl peptidase activity was determined using H-Ala-Pro-pNA substrate. At each time point, the enzyme that was not treated with H_2O_2 or PQQ was used as a control. Mean and SD, n = 3.

Table 2. DP8 Oxidation and Reduction. Samples of 10 μM DP8 were incubated with 0.2 mM PQQ for 1 h at 37°C in 0.1 M pH 7.5 sodium phosphate buffer. The samples were passed through a sephadex-G25 column to remove the PQQ, H_2O_2 and IAA prior to peptidase assay and determination of SH content. SH content was determined in the presence of 6 M guanidine HCl using 5 μM DP8 and 2 mM DTNB

Treatment	Activity (% of Untreated)	SH Residues per Monomer
DP8	100	6
DP8 + IAA (10 mM)	92	4.2
DP8 + H_2O_2 (2 mM)	25	3.8
DP8 + PQQ (0.2 mM)	28	3.9
DP8 + IAA (10 mM) 60 min then H_2O_2 (2 mM)	76	4.0
DP8 + IAA (10 mM) 60 min then PQQ (0.2 mM)	73	3.8

This time course data fitted nonlinear regressions with R values > 0.98. Similar effects were obtained on DP8 and DP9 and no effect on DPIV or FAP were produced using 2 mM dithiothreitol. Based on the interaction between GSH and thiol groups of Cys in DP8 and DP9, thiol affinity chromatography was evaluated as a means of purifying DP8. The yield was about 65%. DP8 was highly purified such that it appeared as a single band in silver stained gels (Fig. **8A**). To investigate the mode of oxidation induced activity modulation, PQQ treated DP8 was applied to SDS-PAGE in the absence of reducing reagent: A gel shift would have been an indication of intermolecular rather than intramolecular disulfide bonds. The mobility of DP8 was similar under oxidized or reduced conditions (Fig. **8B**), so this approach did not detect evidence of altered protein topology.

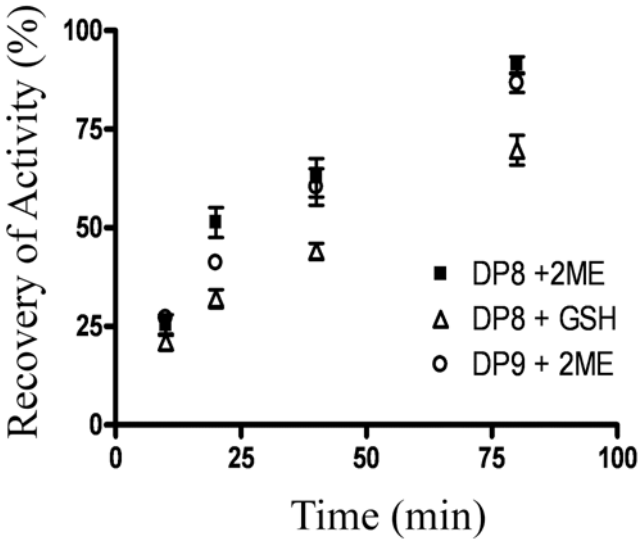

Fig. (7). Time course of reactivation of oxidized DP8 and DP9. Samples of oxidized 10 μM DP8 and 10 μM DP9 were incubated with 2-ME (2 mM) or reduced glutathione (GSH; 5 mM) in sodium phosphate buffer (pH 7.5) at 37°C. Aliquots withdrawn at indicated times were assayed for dipeptidyl peptidase activity using H-Ala-Pro-pNA. Mean and SD, n = 4.

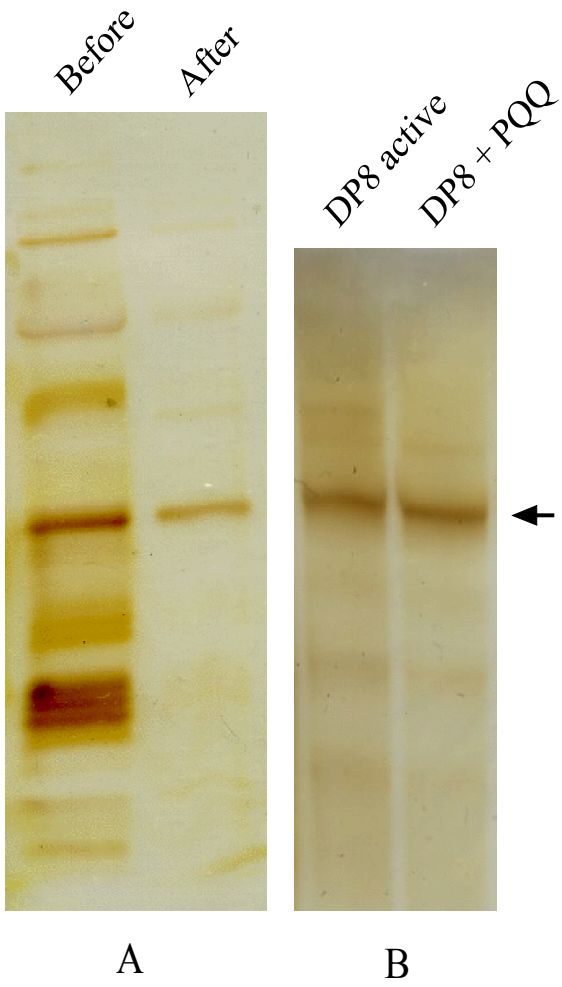

Fig. (8). DP8 thiol affinity purification and DP8 oxidation. **A.** DP8 partially purified by DEAE anion chromatography (Before) was applied to thiol affinity chromatography using Thiol Sepharose 4B (After) then proteins were visualized by silver staining on 8% SDS-PAGE. **B.** 8% nonreducing SDS-PAGE of silver stained purified active DP8, DP8 inactivated by oxidizing with PQQ (0.2 mM). Arrow points to DP8 at 100 kDa.

Cys 3D Locations in DP9 and DP8

The 3D structures of DP9 and DP8 are unknown so relationships with known structures within the DPIV gene family were used to examine potential 3D locations of Cys. Consideration of predicted Cys locations and separation distances (Table **3**, Fig. **9**) led us to propose that reactive cysteines in DP9 and DP8 influence peptidase activity by increasing the rigidity of the tertiary structure. In PEP, catalysis is inhibited by NEM binding to Cys255 because it is sufficiently near to the catalytic pocket to physically exclude substrate [17]. The models of DP9 and DP8 tertiary structure indicated that all Cys residues are further from the catalytic pocket than is Cys255 in PEP. Thus, the models do not support, but neither do they refute, a hypothesis that a Cys in DP9 or DP8 has the same role as the PEP Cys255.

These DP9 and DP8 models concur closely with recently published models [35] except that our sequence alignment differs in the beta-propeller domain. The only significant effect of this is that we model some surface features that are not present in the other models. The catalytic pockets do not differ.

Construction of a disulfide bond in the PEP propeller domain and distant from the catalytic pocket ablates catalytic activity, suggesting that catalytic activity requires β-propeller domain flexibility [36]. Therefore, naturally occurring Cys pairs that might disulfide bond and thus influence propeller domain flexibility were sought in DP9 and DP8. Distances between Cα atoms in Cys pairs are generally 4 to 9 Å and are 4.0 to 6.8 Å in DP4, FAP and DP6. Table **3** lists the Cys pairs that have Cα - Cα distances of 5.6 to 12.9 Å in the DP9 and DP8 models. The potential Cys pairs most distant in primary structure but within 12 Å in 3D models were considered the most likely to influence protein flexibility if they form a disulfide bond. These Cys pairs were residues 683 with 481, 601 with 571 and 162 with 184 in DP9 and 692 with 490 in DP8. The identification of such Cys residues supports the hypothesis that intramolecular disulfide bonds influence structural flexibility in these peptidases. The positions of Cys683 and Cys692 on the α/β-hydrolase domain and Cys481 and Cys490 on the β-propeller domain suggest a further speculation that these Cys pairs might be involved in didomain movement.

Table 3. Intra-Cys Distances < 13 Å in the DP9 and DP8 Models. Disulphide Cys Pairs have Cα-Cα distances of 4 to 9 Å. Larger distances are of interest to allow for localised rearrangements

Cα – Cα Distance (Å)	Cysteine Residue Numbers	
DP9		
5.61	447	452
7.38	162	184
8.07	184	194
9.55	452	481
9.89	447	481
10.69	481	683
11.64	571	601
11.89	452	683
12.19	184	225
12.90	162	194
DP8		
7.82	195	205
10.64	490	692
12.10	456	490
12.39	560	565

DISCUSSION

Some DP8 and DP9 substrates have been identified but the weak kinetics suggests that biologically significant substrates of these enzymes are yet to be discovered [19]. DP8 expression upregulation by activated T cells and T cell proliferation suppression by DP8/9 inhibitors suggests that such substrates and thus a role of DP8/9 may be in immune cells [32, 37]. The present study showed that thiol groups of DP8 and DP9 are targets of oxidation - reduction processes that impact upon enzyme activity. The data indicated that two Cys residues of DP8 and DP9 may be responsible for both alkylation and oxidation induced inactivation.

In protein tyrosine phosphatases oxidation causes disulfide bond formation between two Cys, one in the active site and one nearby. The 3D structure of PEP has shown that in the catalytic pocket of PEP Cys255 is close to the S1 and S3 subsites of the active site such that its alkylation causes some loss of catalytic activity and bulky reagents specific to Cys residues such as NEM and pHMB inactivate PEP almost completely [17]. As in PEP, Cys alkylation of DP8 and DP9 may similarly block substrate access to the active site. However, unlike PEP in which only one Cys is involved, we obtained data that in DP8 and DP9 two Cys are involved and we propose that the disulfide bonding indirectly impedes substrate access to the catalytic pocket by decreasing flexibility in the tertiary structure.

The size of alkylating reagents affects the inhibition of enzyme activity differentially among prolyl oligopeptidase family members: IAA inhibits PEP [16] and DP9 by about 50% but does not inhibit DP8; NEM inhibits PEP [16], DP8 and DP9. Consistent with previous studies [32], alkylation did not influence DPIV activity. Similarly, alkylation did not affect enzyme activity of FAP.

The oxidizing reagents used in this study were H_2O_2 and PQQ. Most protein Cys residues are not sensitive to oxidation by H_2O_2 at neutral pH because the pKa values of most protein Cys-SH residues are >8.0. The nucleophilicity of an –SH group is negligible compared with its ionized form. Occasionally, protein Cys residues exist as thiolate anions at neutral pH when the pKa values of these Cys residues are lowered as a result of interaction between the negatively charged thiolate and the positively charged residues nearby [38]. Unlike DPIV and FAP, DP8 and DP9 were inactivated by H_2O_2 at pH 7.5. This suggests that the enzymes DP8 and DP9 have Cys group(s) with low pKa values consistent with being H_2O_2 sensing proteins.

Residues other than Cys can be oxidized, but the only realistic candidate, methionine, has a rate constant with H_2O_2 at pH 7 of about 10^{-4} $dm^3mol^{-1}s^{-1}$ that is about ten thousand times less than Cys in mammalian H_2O_2 sensor proteins [39, 40]. Moreover, there is no report that methionine is reversibly regulated in protein function such as enzyme activity. Therefore, it is likely that all the observations reported here relate to effects on Cys residues.

Interestingly, the oxidized DP8 and DP9 recover their catalytic activity when treated with reducing agents (2-ME or GSH) (Fig. **7**). The biological role of this oxidation and reduction process and its influence upon enzyme activity needs further investigation including finding biological substrates as well as linkage with corresponding reducing system(s) such as the thioredoxin system or glutaredoxin system. In connection with signal transduction by H_2O_2, modulation of protein activity by disulfide formation is becoming a universal mechanism of protein redox regulation due to its fast and efficient turn-on/off mechanism in cellular signals [4, 6].

In PEP, conformational change is required for catalysis and decreased propeller domain flexibility has been associated with decreased catalysis [36, 41]. Moreover, an open form of PEP, from *Myxococcus xanthus*, has been observed in which the two domains move apart on a hinge [42]. Therefore we speculate that natural intramolecular disulfide bonds in DP9 and DP8 diminish catalysis by decreasing tertiary structure flexibility. Whether DP9 and/or DP8 adopt an open form that is closed at least in part by a disulfide bond is an intriguing possibility suggested by the *M. xanthus* PEP open structure.

H_2O_2 mediated signal transduction occurs in various cell types [2] and a number of proteins are controlled by Cys reduction and oxidation [9]. The ubiquitous expression of DP8 and DP9 [13, 32, 43] means that their regulation is probably important in many organs and biological processes. In addition to the immune system, skin may be an important location for this process; ultraviolet light produces sufficient reactive oxygen species and DP8 and DP9 are abundant in human skin (J. Park, G. Halliday, D. Damian unpublished).

ACKNOWLEDGEMENTS

Supported by Australian National Health and Medical Research Council grants 293803 and 512282 to MDG, a

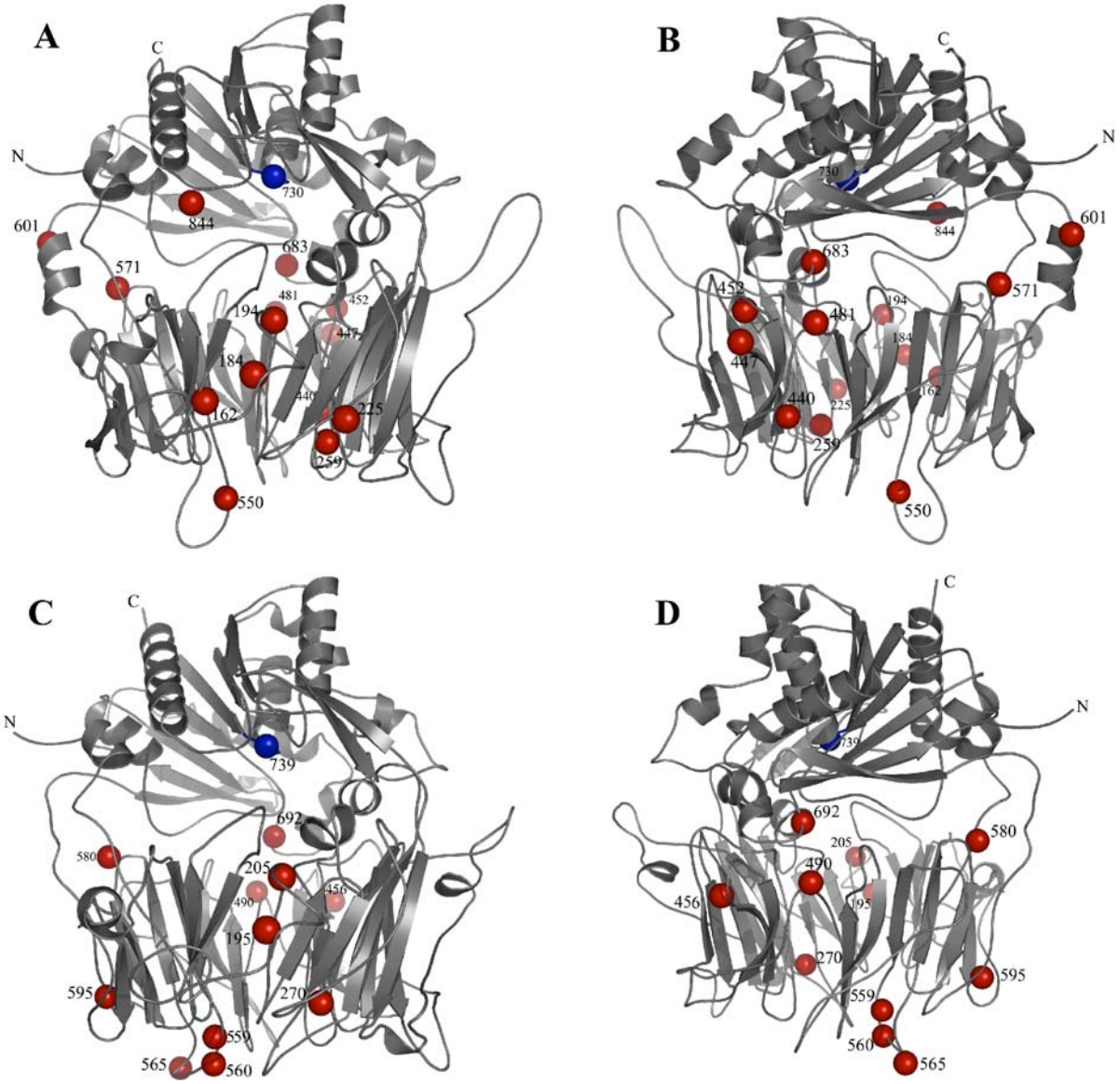

Fig. (9). Cys locations in DP9 and DP8. Models of DP9 (A, B) and DP8 (C, D) are depicted in ribbon representation in side view perpendicular to the pseudosymmetry axis. Cys locations are shown as red spheres and the catalytic Ser as a blue sphere. The 3D structures are oriented similarly in panel C as in A and in panel D as in B, with a 180° rotation of A and C to obtain B and D respectively.

University of Sydney Postgraduate Award to JP and an Australian Postgraduate Award to NAN.

Enzymes: dipeptidyl peptidase IV GenBank P27487, EC 3.4.14.5; prolyl endopeptidase, GenBank P48147, EC 3.4.21.26; dipeptidyl peptidase 8 GenBank AF221634; dipeptidyl peptidase 9 GenBank AY374518; fibroblast activation protein GenBank U09278.

ABBREVIATIONS

AFC	=	7-Amido-4-trifluoromethylcoumarin
DP	=	Dipeptidyl peptidase
DTNB	=	5,5'-Dithiobis(2-nitrobenzoic acid)
FAP	=	Fibroblast activation protein
GSH	=	Reduced glutathione
H_2O_2	=	Hydrogen peroxide
IAA	=	Iodoacetamide
2-ME	=	2-Mercaptoethanol
PEP	=	Prolyl endopeptidase
p-NA	=	p-Nitroanilide
pHMB	=	4-(Hydroxymercuri) benzoate
NEM	=	N-Ethylmaleimide
PQQ	=	Pyrroloquinoline quinone
PTEN	=	Phosphatase and tensin homolog
Suc	=	3-Carboxy-propionyl

REFERENCES

[1] Droge W. Free radicals in the physiological control of cell function. Physiol Rev 2002; 82: 47-95.

[2] Finkel T. Signal transduction by reactive oxygen species in non-phagocytic cells. J Leukoc Biol 1999; 65: 337-40.

[3] Rhee SG. Redox signaling: hydogen peroxide as intracellular messenger. Exp Mol Med 1999; 31: 53-9.
[4] Cho SH, Lee CH, Ahn Y, *et al*. Redox regulation of PTEN and protein tyrosine phosphatases in H2O2 mediated cell signaling. FEBS Lett 2004; 560: 7-13.
[5] Finkel T. Redox-dependent signal transduction. FEBS Lett 2000; 476: 52-4.
[6] Kwon J, Lee SR, Yang KS, *et al*. Reversible oxidation and inactivation of the tumor suppressor PTEN in cells stimulated with peptide growth factors. Proc Natl Acad Sci U S A 2004; 101: 16419-24.
[7] Mahadev K, Zilbering A, Zhu L, Goldstein BJ. Insulin-stimulated Hydrogen Peroxide Reversibly Inhibits Protein-tyrosine Phosphatase 1B *in Vivo* and Enhances the Early Insulin Action Cascade. J Biol Chem 2001; 276: 21938-42.
[8] Forman HJ, Fukuto JM, Torres M. Redox signaling: thiol chemistry defines which reactive oxygen and nitrogen species can act as second messengers. Am J Physiol Cell Physiol 2004; 287: C246-56.
[9] Hogg PJ. Disulphide bonds as switches for protein function. Trends Biochem Sci 2003; 28: 210-4.
[10] Gorrell MD. Dipeptidyl peptidase IV and related enzymes in cell biology and liver disorders. Clin Sci 2005; 108: 277-92.
[11] Thornberry NA, Weber AE. Discovery of JANUVIA (Sitagliptin), a selective dipeptidyl peptidase IV inhibitor for the treatment of type 2 diabetes. Curr Top Med Chem 2007; 7: 557-68.
[12] Wang XM, Yao T-W, Nadvi NA, Osborne B, McCaughan GW, Gorrell MD. Fibroblast activation protein and chronic liver disease. Front Biosci 2008; 13: 3168-80.
[13] Ajami K, Abbott CA, McCaughan GW, Gorrell MD. Dipeptidyl peptidase 9 has two forms, a broad tissue distribution, cytoplasmic localization and DPIV-like peptidase activity. Biochim Biophys Acta 2004; 1679: 18-28.
[14] Dobers J, Grams S, Reutter W, Fan H. Roles of cysteines in rat dipeptidyl peptidase IV/CD26 in processing and proteolytic activity. Eur J Biochem 2000; 267: 5093-100.
[15] Rasmussen HB, Branner S, Wiberg FC, Wagtmann N. Crystal structure of human DPP-IV/CD26 in complex with a substrate analogue. Nat Struct Biol 2003; 10: 19-25.
[16] Polgar L. pH-dependent mechanism in the catalysis of prolyl endopeptidase from pig muscle. Eur J Biochem 1991; 197: 441-7.
[17] Fülop V, Bocskei Z, Polgar L. Prolyl oligopeptidase - an unusual beta-propeller domain regulates proteolysis. Cell 1998; 94: 161-70.
[18] Ellman GL. Tissue sulfhydryl groups. Arch Biochem Biophys 1959; 82: 70-7.
[19] Ajami K, Pitman MR, Wilson CH, *et al*. Inflammatory protein-10, interferon-inducible T cell chemo-attractant and stromal cell-derived factors 1α and 1β are novel substrates of dipeptidyl peptidase 8. FEBS Lett 2008; 582: 819-25.
[20] Levy MT, McCaughan GW, Abbott CA, *et al*. Fibroblast activation protein: a cell surface dipeptidyl peptidase and gelatinase expressed by stellate cells at the tissue remodelling interface in human cirrhosis. Hepatology 1999; 29: 1768-78.
[21] Ajami K, Abbott CA, Obradovic M, Gysbers V, Kähne T, McCaughan GW, Gorrell MD. Structural requirements for catalysis, expression and dimerisation in the CD26/DPIV gene family. Biochemistry 2003; 42: 694-701.
[22] Strop P, Bankovich AJ, Hansen KC, Garcia KC, Brunger AT. Structure of a human A-type potassium channel interacting protein DPPX, a member of the dipeptidyl aminopeptidase family. J Mol Biol 2004; 343: 1055-65.
[23] Aertgeerts K, Levin I, Shi L, *et al*. Structural and kinetic analysis of the substrate specificity of human fibroblast activation protein Alpha. J Biol Chem 2005; 280: 19441-4.
[24] Berman HM, Westbrook J, Feng Z, *et al*. The Protein Data Bank. Nucleic Acids Res 2000; 28: 235-42.
[25] Abbott CA, Gorrell MD. The family of CD26/DPIV and related ectopeptidases. In Ectopeptidases: CD13/Aminopeptidase N and CD26/Dipeptidylpeptidase IV in Medicine and Biology (Langner J, Ansorge S, eds), 2002; pp. 171-95. Kluwer/Plenum, NY.
[26] Sali A, Blundell TL. Comparative protein modeling by satisfaction of spatial restraints. Mol Biol 1993; 234: 779-815.
[27] Laskowski RA, MacArthur MW, Moss DS, Thornton JM. PROCHECK: a program to check the stereochemical quality of protein structures. J Appl Crystallogr 1993; 26: 283-91.
[28] Iwaki-Egawa S, Watanabe Y, Fujimoto Y. N-terminal amino acid sequence of the 60-kDa protein of rat kidney dipeptidyl peptidase IV. Biol Chem Hoppe Seyler 1993; 374: 973-5.
[29] Abbott CA, McCaughan GW, Levy MT, Church WB, Gorrell MD. Binding to human dipeptidyl peptidase IV by adenosine deaminase and antibodies that inhibit ligand binding involves overlapping, discontinuous sites on a predicted beta propeller domain. Eur J Biochem 1999; 266: 798-810.
[30] Chien C-H, Huang L-H, Chou C-Y, *et al*. One site mutation disrupts dimer formation in human DPP-IV proteins. J Biol Chem 2004; 279: 52338-45.
[31] DeLano WL. The PyMOL molecular graphics system, 2002; DeLano Scientific. San Carlos, CA, USA.
[32] Abbott CA, Yu DMT, Woollatt E, Sutherland GR, McCaughan GW, Gorrell MD. Cloning, expression and chromosomal localization of a novel human dipeptidyl peptidase (DPP) IV homolog, DPP8. Eur J Biochem 2000; 267: 6140-50.
[33] Park J, Churchich JE. Pyrroloquinoline quinone (coenzyme PQQ) and the oxidation of SH residues in proteins. Biofactors 1992; 3: 257-60.
[34] Park J, Churchich JE. Interaction of thioredoxin with oxidized aminobutyrate aminotransferase. Evidence for the formation of a covalent intermediate. FEBS Lett 1992; 310: 1-4.
[35] Rummey C, Metz G. Homology models of dipeptidyl peptidases 8 and 9 with a focus on loop predictions near the active site. Proteins 2007; 66: 160-71.
[36] Fülop V, Szeltner Z, Polgar L. Catalysis of serine oligopeptidases is controlled by a gating filter mechanism. EMBO Reports 2000; 1: 277-81.
[37] Lankas G, Leiting B, Roy R, *et al*. Dipeptidyl peptidase IV inhibition for the treatment of type 2 diabetes - Potential importance of selectivity over dipeptidyl peptidases 8 and 9. Diabetes 2005; 54: 2988-94.
[38] Lee SR, Yang KS, Kwon J, Lee C, Jeong W, Rhee SG. Reversible inactivation of the tumor suppressor PTEN by H2O2. J Biol Chem 2002; 277: 20336-42.
[39] Davies MJ. The oxidative environment and protein damage. Biochim Biophys Acta 2005; 1703: 93-109.
[40] Stone JR. An assessment of proposed mechanisms for sensing hydrogen peroxide in mammalian systems. Arch Biochem Biophys 2004; 422: 119-24.
[41] Szeltner Z, Rea D, Juhasz T, Renner V, Fulop V, Polgar L. Concerted structural changes in the peptidase and the propeller domains of prolyl oligopeptidase are required for substrate binding. J Mol Biol 2004; 340: 627-37.
[42] Shan L, Mathews II, Khosla C. Structural and mechanistic analysis of two prolyl endopeptidases: Role of interdomain dynamics in catalysis and specificity. Proc Natl Acad Sci U S A 2005; 102: 3599-604.
[43] Qi SY, Riviere PJ, Trojnar J, Junien JL, Akinsanya KO. Cloning and characterization of dipeptidyl peptidase 10, a new member of an emerging subgroup of serine proteases. Biochem J 2003; 373: 179-89.

Received: April 15, 2008 Revised: May 20, 2008 Accepted: May 20, 2008